Testing and modeling of damages in composite laminates subject to low velocity impact

Al-Hadrayi Ziadoon M. R, Zhang Yunlai, Zhou Chuwei

State Key Laboratory of Mechanics and Control of Mechanical Structures, Nanjing University of Aeronautics and Astronautics, 29Yudao Street 210016, Nanjing, China.

Abstract
In recent years, composite materials were used extensively in the most important industries, especially in aerospace industries and aircraft structures due to its high strength, high stiffness, resistance of corrosion, and lightweight. The problem is how to choose the perfect design for composite laminates. And study the effects of modeling of the stacking sequences of composite laminates on failure modes (delamination, matrix cracking, and fiber failure) under the test of low velocity impact. This paper has validating to the experimental results that has published. The composite used was carbon fiber /epoxy (CFRE), (UD ASTM/D6641) as three groups [A, B, C]. It had same material system. The difference was only in stacking sequences as random design. These models were simulated numerically by the commercial software implemented into the FEM/ABAQUS 6.9.1 with subroutine file (VUMAT) a user-define 3D damage model. The results had good agreement with experimental results.

Keywords: Composite laminates; Stacking sequences; Low velocity impact; Delamination.

1. Introduction
One of the most important critical factors of the loading for composite laminates is a test of low-velocity impact. The studying of the test of low velocity impact on structures of composite materials since 1970s the response of laminates structural differs between the tests of high and low velocity impacts. For the test of high velocity impact, the event is very short so that the laminates structural may have not enough time to respond in shear modes or and flexural. While for the test of low velocity impact, the contact duration is enough fully to the entire structure for respond under the impact and the absorbed energy may have elastically or eventually in the damage creating [2]. The damages are divided to three types (delamination, matrix cracking, and fiber failure) due to the loading of impact. Collombet [3] the interface element has been used by a simple test in normal stress. The opening of the first fracture mode compared with the fraction of second and third. So it is hard to be experimentally tested this hypothesis. Vlot [4] Compared with sufficient energy to create different types of cracks in the FMLs under low velocity impact, and found that the FMLs with fiberglass need higher energy FMLs with aramid or carbon fiber, although both types of FMLs comparable data with the composites plane. Abrate S [5] had been discovered of the brittle behavior of composite materials in terms of damage (cracking of matrix, delamination, and fiber failure. These damages are dangerous because it reduces the residual mechanical properties for structure, and at the same time limited leave visible marks on the impact surface. Berbinua [6, 7] had been described the behavior of nonlinear shear for laminate. Her and Liang [8] they are

using ANSYS/LS-DYNA investigated the effect of the curvature of shell, impactor velocity and the boundary condition on composite laminates of graphite/epoxy under low velocity impact. The results were obtained showed the force of contact is proportional to impactor velocity. Pinho [9] used the tests of compact compression to evaluate the kinetic fracture of T300/913 carbon epoxy laminates. Had been used the energy criterion for matrix cracking and failure of fiber in 3D in their damage model of low velocity impact with evaluation law of the exponential for damage propagation. Abdullah [10] had been using fiber metal laminates and found that FMLs absorb the energy impact through the aluminum plastic deformation and composite, Also the micro-cracking in the layers of composite. Shi Y [11] had been simulated of damage development by using a simple cross ply $[0, 90]_{2s}$. The failure criterion to predict initiation of damage is a stress based failure criterion while the energy criterion was using it to simulated cracking of intra-and inter laminar. Gonzalez [12] had been suggested a model can be able to simulate impact and compression after impact (CAI) tests. In this model, constitutive material models were used for calculations of the ply failure mechanics and delamination models formulated in the context of continuum damage mechanics. It is difficult to compare with the experimental data due to lack of knowledge of CAI's damage is obtained experimentally. Taheri-Behrooz [13] had been studying the effect of the stacking sequences on the impact behavior of FMLs that was evaluated in the terms of the capacity of load-carrying and the mechanism failure. The numerical model was implemented by using ABAQUS 6.9 software. The comparison was between the numerical simulation result and experimental results but did not show that the failure modes in the simulation and compared it with experimental results. Chirangivee [14] had studied the effect the stacking sequences on impact behavior by using glass fiber reinforced plastic. From the results that were obtained, found the maximum force of contact was change with increasing the energy impact for equal velocity and equal mass and there are not any compared between the failures modes of the simulation and the experiment. So in this paper will be compared the failure modes of the simulation and the experimental results of previous paper et al. [1].

2. Numerical and FEM modelling
2.1 Impact loading
Mindlin plate element takes the deformation of transverse shear and the significant deformation are given in account and it has five degrees of freedom system on each node [u_i, v_i, w_i, ϑ_{xi}, ϑ_{yi}] [15], because of the low-cost of computational and potent ability. Equation of motion of a system can be written as the following to describe the dynamic system:

$$[M]\{\ddot{U}\}+[K]\{U\}=\{P\}-\{F\} \tag{1}$$

Figure 1 illustration the impact model as a mass (m) is rigid ball, has velocity (v) impact at the center of the composite laminates. The dynamic equation can be written as following for rigid ball,
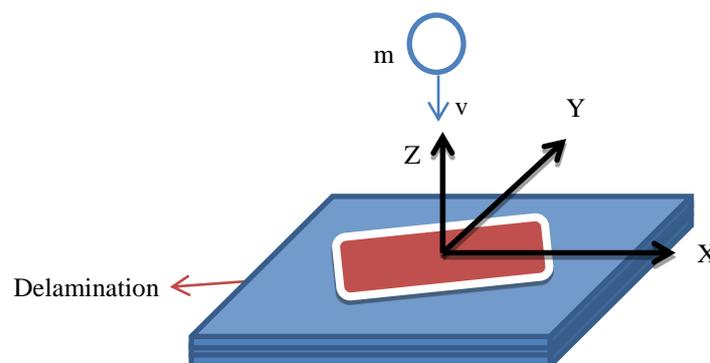
$$m\dot{v}=f-mg \tag{2}$$

Figure 1. Impact model.

By using the modified law of the Hertz theory [16] to calculate the reaction force and depth of indentation due to the impact the ball at the center of surface laminates composite .so it can be written as:

$$F = \begin{cases} k\alpha^{1.5} & \text{loading} \\ Fm\left(\frac{\alpha-\alpha 0}{\alpha m-\alpha 0}\right)^q & \text{unloading} \end{cases}$$

$$\alpha = \begin{cases} \beta(\alpha m - \alpha cr) & (\alpha m > \alpha cr) \\ 0 & (\alpha m \leq \alpha cr) \end{cases} \qquad (3)$$

2.2 Modelling failure modes
2.2.1 Modelling of fiber and matrix failure
Some authors [17-20] deal with different types of failure. In this study, Hashin's Failure criterion was used [21, 22]. Table 1 contents the strategy of the failure according to that criterion. This criterion of fiber and matrix failure can be written as following

a) Tensile fiber failure

$$\left(\frac{\sigma 1}{Xt}\right)^2 + \frac{\tau 12^2 + \tau 13^2}{S12} = \begin{cases} \geq 1 \ failure \\ < 1 \ no \ failure \end{cases}$$

b) Compressive fiber failure

$$\left(\frac{\sigma 1}{Xc}\right)^2 = \begin{cases} \geq 1 \ failure \\ < 1 \ no \ failure \end{cases}$$

c) Tensile matrix failure

$$\frac{\sigma 2^2 + \sigma 3^2}{Yt^2} + \frac{\tau 23^2 - \sigma 2\sigma 3}{S23^2} + \frac{\tau 12^2 + \tau 13^2}{S12^2} = \begin{cases} \geq 1 \ failure \\ < 1 \ no \ failure \end{cases} \qquad (4)$$

d) Compressive matrix failure

$$\left[\left(\frac{Yc}{2S23}\right)^2 - 1\right]\left(\frac{\sigma 2+\sigma 3}{Yc^2}\right) + \frac{\sigma 2+\sigma 3}{4S23^2} + \frac{\tau 23^2 - \sigma 2\sigma 3}{S23^2} + \frac{\tau 12^2 + \tau 13^2}{S12^2} = \begin{cases} \geq 1 \ failure \\ < 1 \ no \ failure \end{cases}$$

A process of progressive failure analysis of composite structures for any types of loading requires both a stress analysis model of laminates and failure modes. After the stresses concentration in each layer of composite material layers are defined in the laminates analysis. Laminate failure is expected be either using the standard failure phenomena or the stress in each laminate consisting of composite components. Criterion of failure is used to determine the extent of the matrix cracking and damage of core plus the delamination. The results of failure are compared with the results that were obtained in the experiment.

Table 1. Strategy of degradation method.

Failure modes	Degradation method
Tensile matrix failure	$E_{22} = 0.2E_{22}, G_{12} = 0.2G_{12}, G_{23} = 0.2G_{23}$
Compressive matrix failure	$E_{11} = 0.4E_{22}, G_{12} = 0.4G_{12}, G_{13} = 0.4G_{13}$
Tensile fiber failure	$E_{x11} = 0.01E_{11}, G_{12} = 0.01G_{12}, G_{13} = 0.01G_{13}$
Compressive fiber failure	$E_{11} = 0.01E_{11}, G_{12} = 0.01G_{12}, G_{13} = 0.01G_{13}$

2.2.2 Modelling of delamination
The analysis of damage in composite materials under low velocity impact can be classified into two types: Damage mechanics and fracture mechanics. Damage mechanical model or progressive deterioration, it is the description of variables in the case of damage. On the other side is the fracture mechanics, it is a crack first then the damage begins growth cracks in laminates of composites. Usually, it was used the strain energy criterion (Griffith) to the prediction of crack growth. These classifications of the standards for the analysis are usually very different. This is often requires a smaller scale in cracks in case of fracture mechanics. Delamination damage is very danger damage and it is negatively affecting on the response of composite structure. In Figure 2 shows the model FEM mesh for laminates $0^0/90^0/0^0$ subject to the test of low velocity impact. According to Hashin's criterion can be expressed as,

$$\left(\frac{\sigma 3}{Zt}\right)^2 + \frac{\tau 12^2 + \tau 13^2}{S23^2} = \begin{cases} \geq 1 \ failure \\ < 1 \ no \ failure \end{cases} \qquad (5)$$

While in this paper, it has used Choi-chang [17] failure criterion and the modified model as follows equations,

$$D_\alpha \left[K \left(\frac{\tau_{13}^n}{S_i} \right)^2 + K \left(\frac{\tau_{23}^n}{S_i} \right)^2 + \left(\frac{\sigma_2^{n+1}}{Y_i} \right)^2 \right] \geq 1$$

$$K = \begin{cases} \left(1 + \frac{\sigma_3^n + \sigma_3^{n+1}}{2Y_t} \right)^\beta & \text{if } \sigma_3 \geq 0 \\ \left(1 - \frac{\sigma_3^n + \sigma_3^{n+1}}{2Y_c} \right)^\beta & \text{if } \sigma_3 < 0 \end{cases}$$
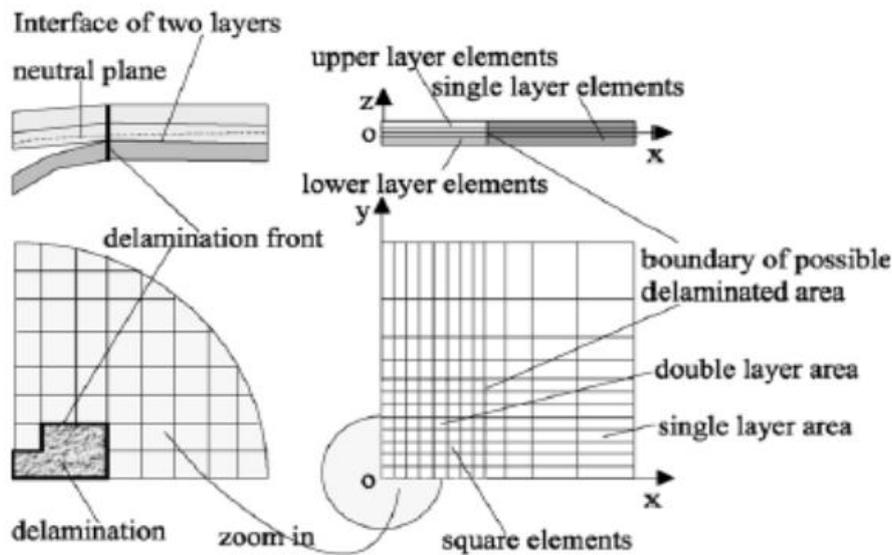
(6)

Figure 2. The FEM delamination model [23].

3. Experimental methods

The specimens are manufactured according to carbon fiber /epoxy (CFRE), (UD ASTM/D6641) as three groups [A, B, C]. It had same material system. The difference was only in stacking sequences as random to validate the effect of stacking sequences on failure modes by using random design of laminates, it was not standard design. The total numbers of the specimens were (18) to get more accurate results, as shown in Figure 3. It was each two specimens for one of the impact energy. The tests were a drop weight (5.5) kg on the center of surface composite laminates caused three impact energy (15, 25 and 35) J. Table 2 [1] contains all the details that were required in the tests of low velocity impact. The dimensions of the specimen were (100*150) mm. Table 3 [1] contains the design of stacking sequences as three groups (A, B, C). The manufacturing was according to 0°, 90°, 45° and -45°.

Table 2. Details of impact test system [1].

Impact energy (J)	Impactor mass(kg)	Impactor velocity(ms^{-1})	Drop height (mm)	Diameter of impactor(mm)	Notes
15		2.3355	278		
25	5.5	3.01511	463.34	16	For every composite
35		3.5675	648.688		

Table 3. Design of stacking sequences for composite materials [1].

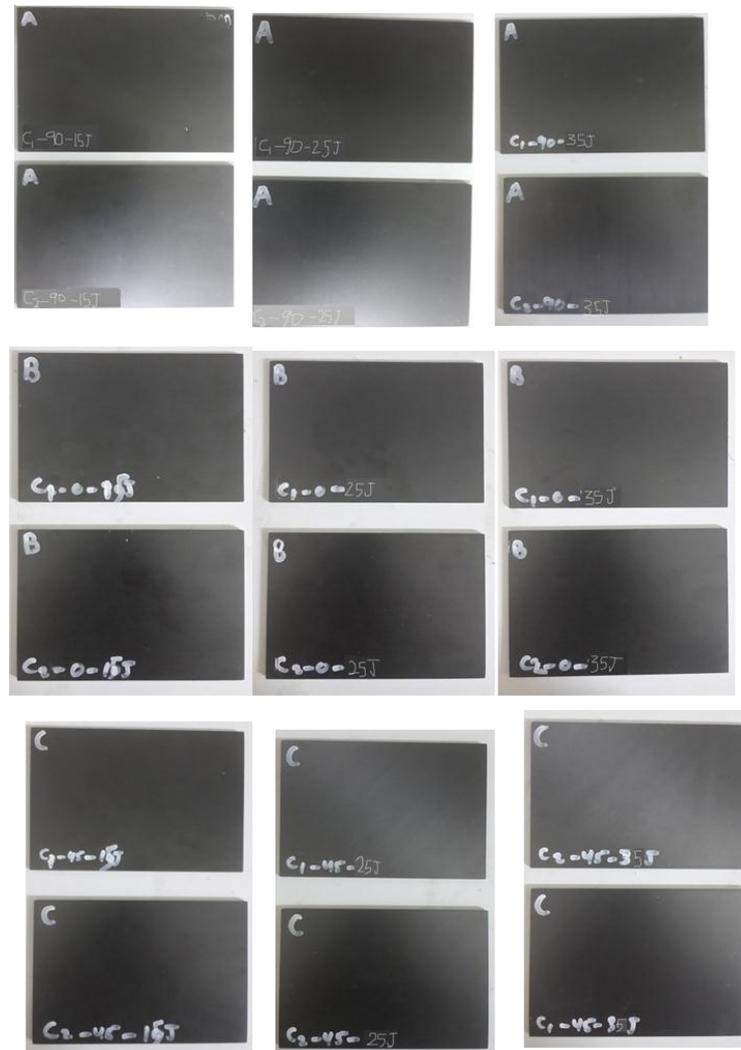| Layup name	Stacking sequences	Plies	Dimensions mm	Thickness mm(average)
A	$[90_2,-45_2,0_2,45_2]_{2s}$			4.2575
B	$[0_2, 45_2,-45_2,90_2]_{2s}$	32	150*100	4.32
C	$[45_2,0_2,90_2,-45_2]_{2s}$			4.48

Figure 3. Specimens of carbon/fiber-epoxy [1].

4. Finite element simulation implemented into the FEM/ABAQUS 6.9.1.

The Modelling was implemented into the commercial software FEM/ABAQUS 6.9.1 according the theory and user's manual [24, 25] to describe the damage of composite model, with subroutine file (VUMAT) a user-define 3D damage model. The analysis of Modelling have consisted two parts as shown in Figure 4, the impactor and composite material. The diameter of impactor was 16 mm. By using C3D8R elements was supported into FEM/ABAQUS 6.9.1. The mesh was hex shape with sweep technique and the algorithm of medial axis. The approximate of global size was five in the sizing controls of global seeds. The first part of the model is the impactor and the second is the surface of composite material. The contact was between the first part (impactor) and the second surface (composite material) during period time was 0.005 (s). Table 4 contains all the mechanical properties that were used into the simulation.
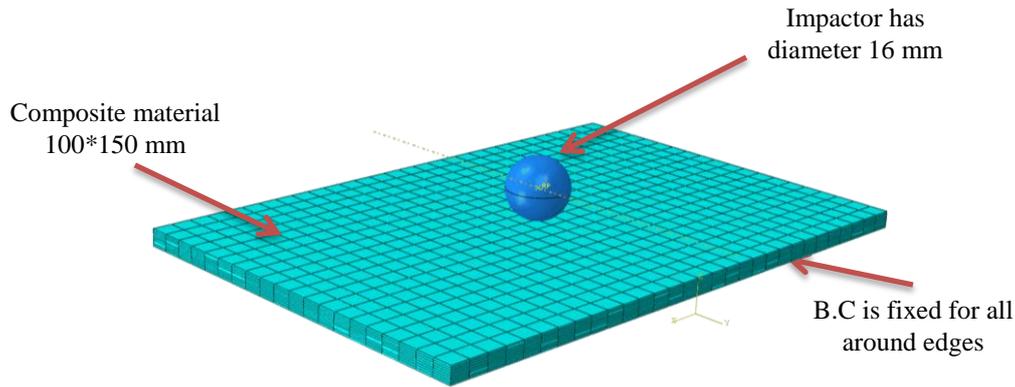
Figure 4. Model of impact, in numerical model three composite with different stacking sequences A $[90_2, -45_2, 0_2, 45_2]_{2s}$, B $[0_2, 45_2, -45_2, 90_2]_{2s}$ and C $[45_2, 0_2, 90_2, -45_2]_{2s}$.

Table 4. Mechanical properties of carbon fiber /epoxy (CFRP), (UD ASTM/D6641) as input in simulation.

symbol	Value
E_{11}	133.58
$E_{22} = E33$	9.25
$G_{12} = G_{13}$	4.32
G_{23}	3.2
$\upsilon_{12} = \upsilon_{13}$	0.3
υ_{23}	0.32
X_t	1368.25
X_c	1068.25
Y_t	178.42
Y_c	211
$S_{12} = S_{13}$	54
S_{23}	50
ρ	1.78

5. Results and discussion

All the models have implemented into the commercial software FEM/ABAQUS 6.9.1 in order to build damage model of composite material subject to the test of low velocity impact. The composites are according to the carbon fiber /epoxy (CFRP), (ASTM/D6641) as three groups [A, B, C]. The carbon volume content of the test material was 91~94%. The results of models are shown as following,

5.1 Delamination

The different shapes of damages have been obtained due to the effect of stacking sequences on failure modes. The shapes are at the left in Figure 5, these were the delamination that was obtained from the previous paper [1]. While the shapes at the right are the delamination of the models that have gotten from the FEM/ABAQUS6.6.

Figure 6 indicates the damages in the different layers at impact 35 J. It can be observed the damages between layers of composite. Laminates damages of composites A & C are less than laminate damage of composite B.

In Figure 7, it has comparison between the numerical delamination area and the experimental delamination area. By using the calculations and the statistics, the errors are as shown in Table (5).

Those results of previous paper [1]

The scale of each element 5*5 mm

A

B

C

(a)

(b)

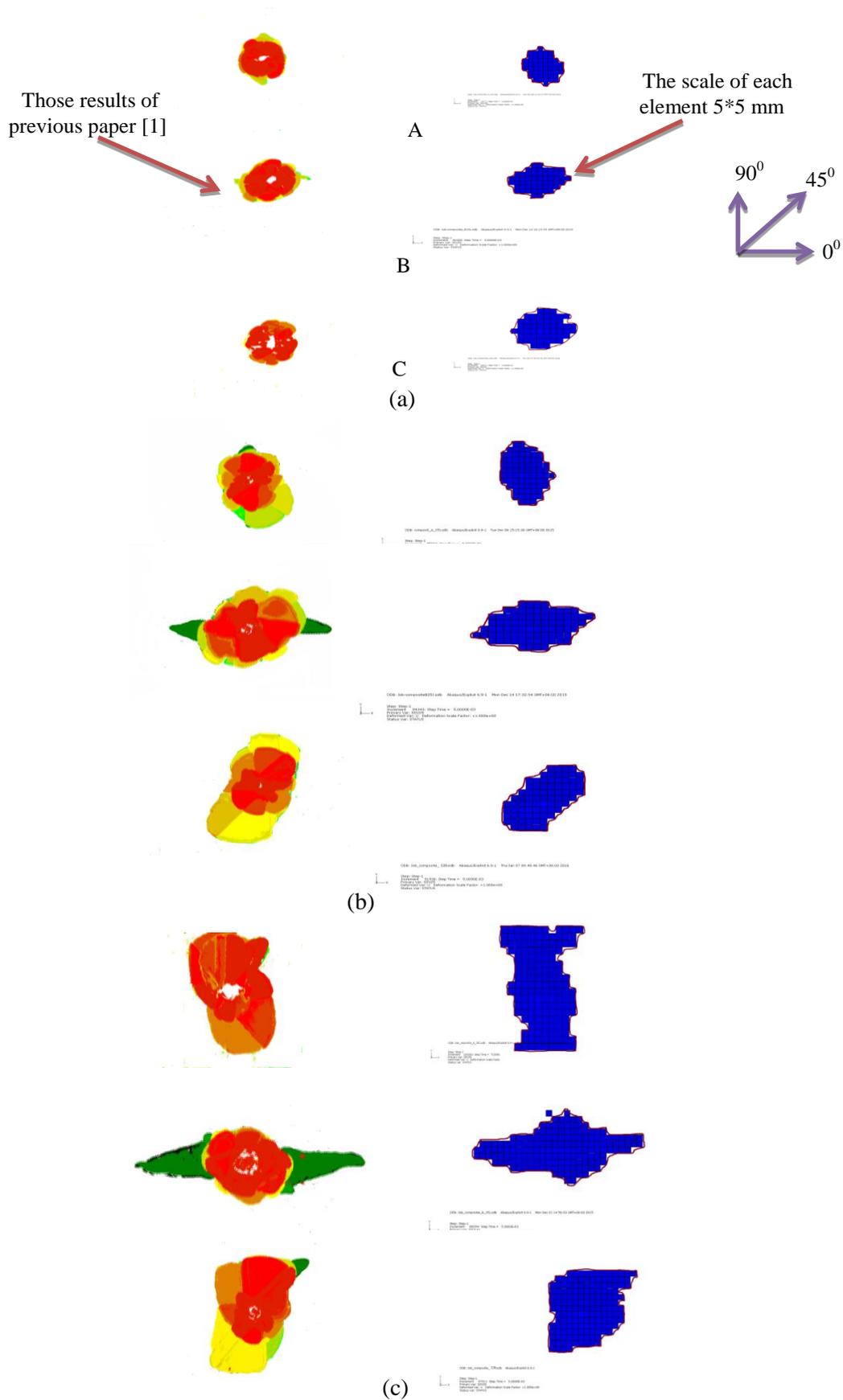(c)

90^0 45^0 0^0

Figure 5. Numerical models of the total delamination compared with experimental results (a) impact energy 15 J, (b) impact energy 25J and (c) impact energy 35J. ((**A** [90_2, -45_2, 0_2, 45_2]$_{2s}$), (**B** [0_2, 45_2, -45_2, 90_2]$_{2s}$), (**C** [45_2, 0_2, 90_2, -45_2]$_{2s}$)).
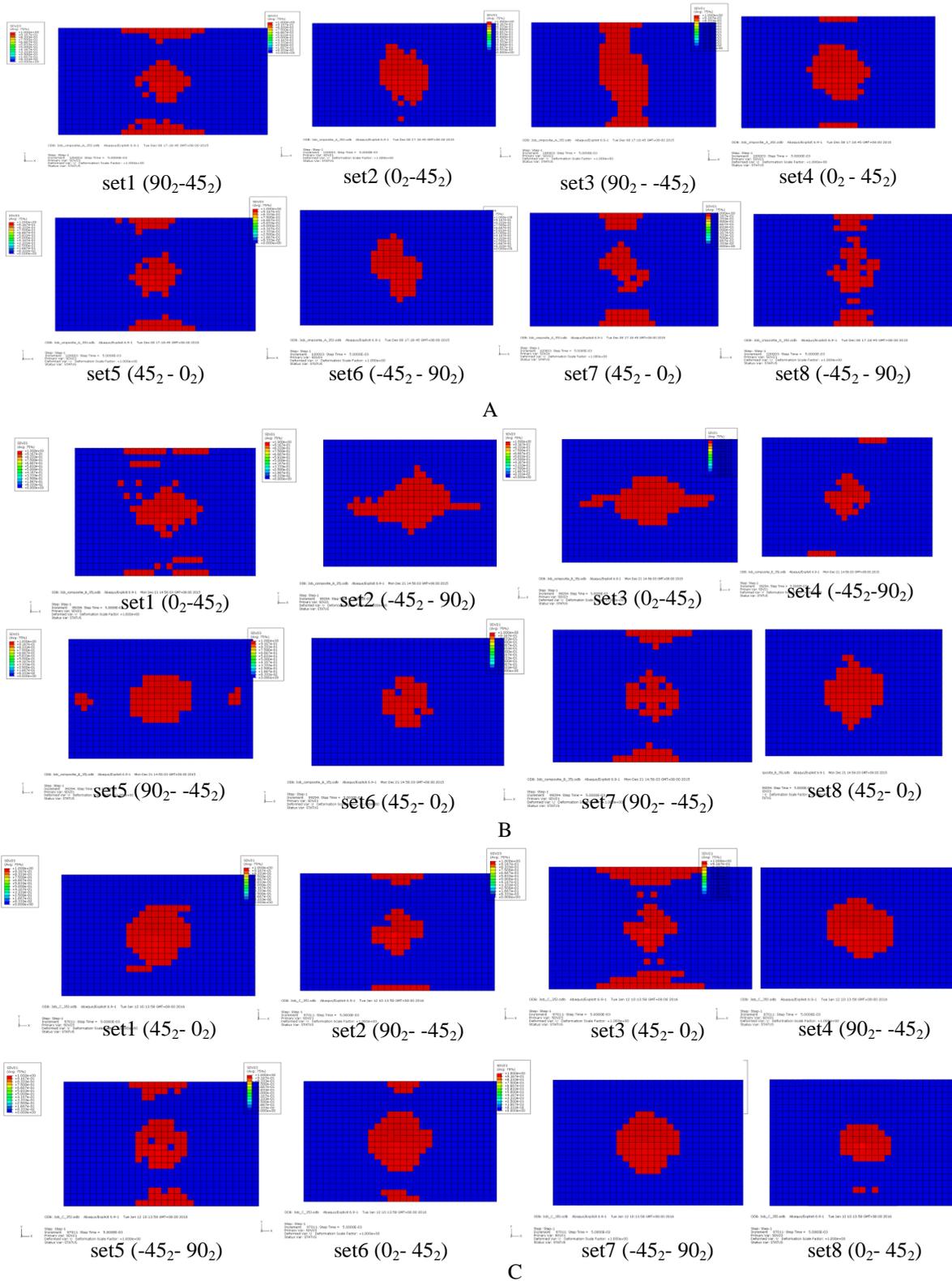
Figure 6. Numerical simulation of delamination damage for various layers at impact energy 35 J as carbon fiber/epoxy in different layups A [90_2, -45_2, 0_2, 45_2]$_{2s}$), B [0_2, 45_2, -45_2, 90_2]$_{2s}$), (C [45_2, 0_2, 90_2, -45_2]$_{2s}$).
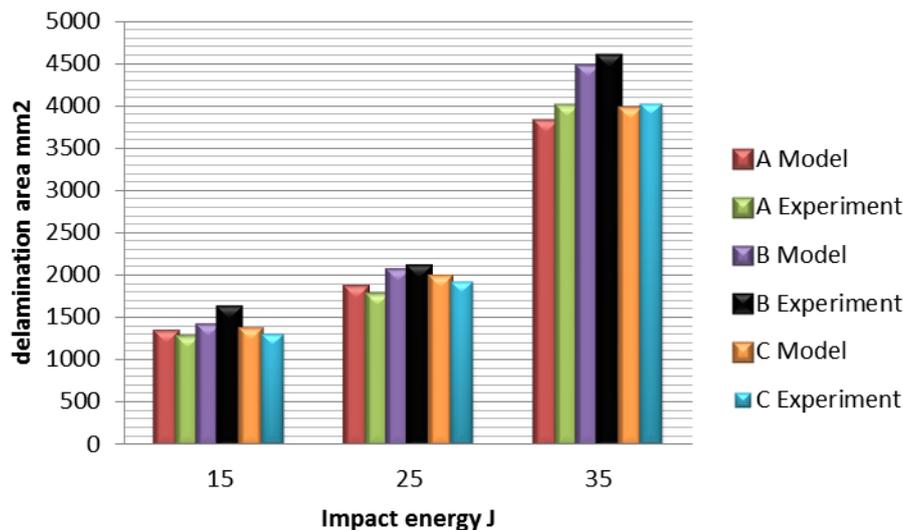
Figure 7. Numerical – Experiment comparison of three different layups in the damage of delamination.

Table 5. Presents the errors percentage in the delamination area according to the comparison between the numerical and experimental (a) impact energy 15 J, (b) impact energy 25J and (c) impact energy 35J.

a	
layups	Error %
A $[90_2,-45_2,0_2,45_2]_{2s}$	5.07
B $[0_2, 45_2,-45_2,90_2]_{2s}$	13.4
C $[45_2,0_2,90_2,-45_2]_{2s}$	3.92
b	
layups	Error %
A $[90_2,-45_2,0_2,45_2]_{2s}$	5.17
B $[0_2, 45_2,-45_2,90_2]_{2s}$	1.86
C $[45_2,0_2,90_2,-45_2]_{2s}$	2.59
c	
layups	Error %
A $[90_2,-45_2,0_2,45_2]_{2s}$	4.49
B $[0_2, 45_2,-45_2,90_2]_{2s}$	2.28
C $[45_2,0_2,90_2,-45_2]_{2s}$	1.9

5.2 Internal energy
Numerically, the internal energy-time history is presented in Figure 8. This figure has indicated the effect of stacking sequences on the internal energy distributed between [A, B, C]   at impact energy (35J). The maximum value of internal energy of composite A & C was more than internal energy of composite B. the internal energy was completely transferred through the impact energy when the velocity reached to the zero. However the results of internal energy were pretty clear to show the effect of stacking sequences as numerically.

5.3 Contact force
The contact was surface to surface. The first surface is the impactor as rigid ball, its diameter 16 mm. while the second surface is the surface of plate (impacted plate). That contact has defined into ABAQUS/Explicit by the general of algorithm contact. Figure 9 has presented the numerical impact force-time history at impact energy 35 J. It shows the composites A&C are stiffer than composite B. The interval time was from 0 to 5ms during the impact. While Figure 10 represents the maximum value of impact force vs the impact energy at the equal mass of impactor which it was about 5.5 kg and it's compared between the composites [A, B, C]. It can be observed that the composites A&C were stiffer than composite B. Figure 11 has indicated the stresses distribution at impact energy 35 J. Composites A&C have values of stresses large than composite B.
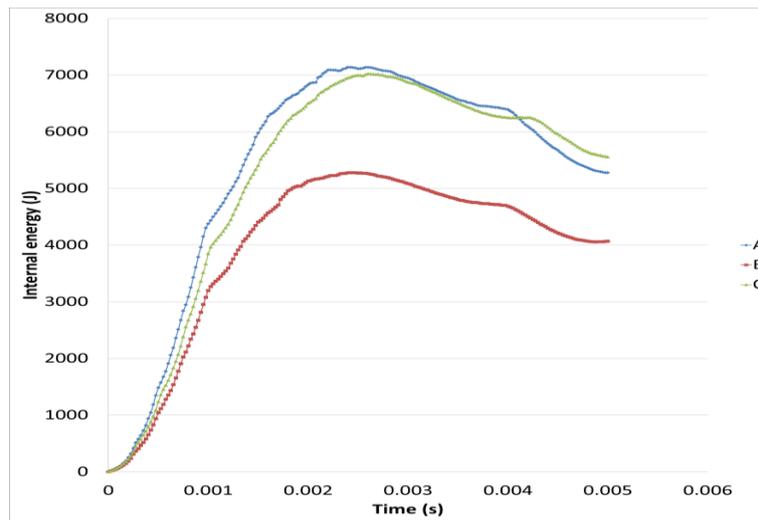
Figure 8. Numerical the internal energy-time histories at impact energy 35 J (A $[90_2, -45_2, 0_2, 45_2]_{2s}$, B $[0_2, 45_2,-45_2, 90_2]_{2s}$, C $[45_2, 0_2, 90_2, -45_2]_{2s}$).
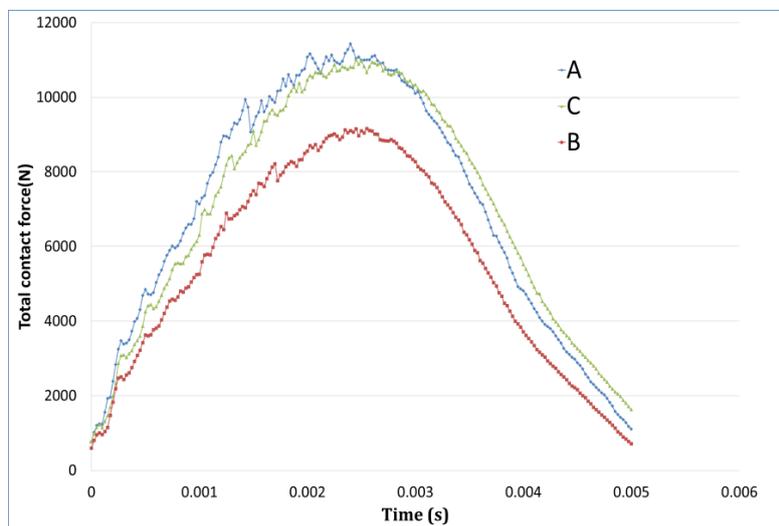

Figure 9. Numerical the total force-time histories at impact energy 35 J (A $[90_2, -45_2, 0_2, 45_2]_{2s}$, B $[0_2, 45_2,- 45_2, 90_2]_{2s}$, C $[45_2, 0_2, 90_2, -45_2]_{2s}$).
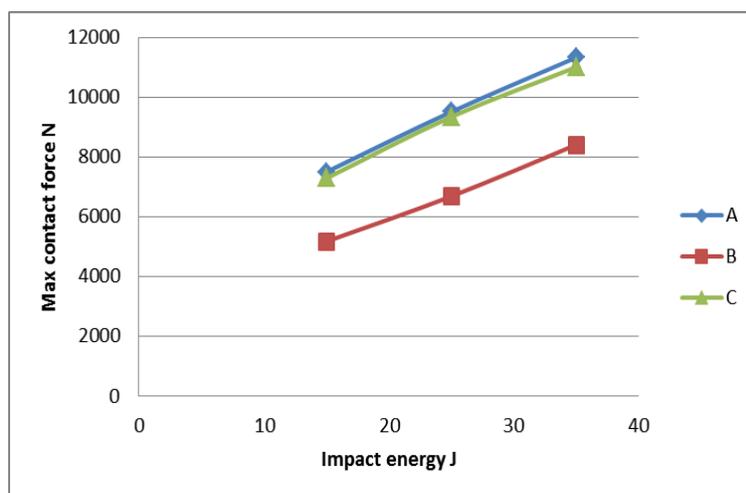

Figure 10. Numerical the maximum impact force vs. impact energy(15, 25, 35) J at equal mass of impactor 5.5 kg (A $[90_2, -45_2, 0_2, 45_2]_{2s}$, B $[0_2, 45_2, -45_2, 90_2]_{2s}$, C $[45_2, 0_2, 90_2, -45_2]_{2s}$).
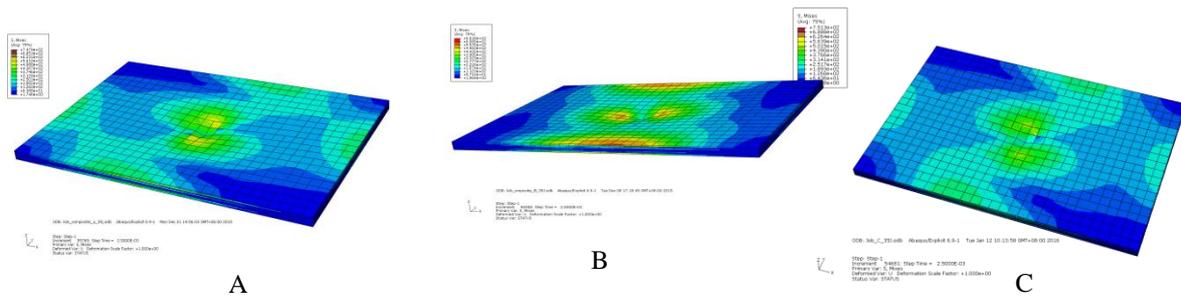
A   B   C

Figure 11. Stress contours for composite plate at impact energy 35 J for carbon fiber/epoxy (A [90_2, -45_2, 0_2, 45_2]$_{2s}$), (B [0_2, 45_2, -45_2, 90_2]$_{2s}$), (c) (C [45_2, 0_2, 90_2, -45_2]$_{2s}$).

5.4 Matrix cracking

The numerical models of matrix cracking have indicated the damages that were predicted within different layers. In Figure 12 can observed the damages of matrix cracking between the various laminates. Those damages were predicted by using the strategy and the technique of degradation in Table 1. The damages distribution, the largest area of damage was at the ordination (90° and 0°) especially in the composite A & B. The red color was the tensile matrixes cracking while the blue color was compressive matrix cracking. The results had observed the composite B was higher damage matrix cracking more than composites of A&C.

set1 (90_2- -45_2)   set2 (0_2- 45_2)   set3 (90_2- -45_2)   set4 (0_2- 45_2)

set5 (45_2- 0_2)   set6 (-45_2- 90_2)   set7 (45_2- 0_2)   set5 (-45_2- 90_2)

(a)

set1 (0_2- 45_2)   set2 (-45_2- 90_2)   set3 (0_2- 45_2)   set4 (-45_2- 90_2)

set5 (90_2- -45_2)   set6 (45_2- 0_2)   set7 (90_2- -45_2)   set1 (45_2- 0_2)

(b)

Figure 12. Continued.

set1 (45$_2$- 0$_2$)   set2 (90$_2$- -45$_2$)   set3 (45$_2$- 0$_2$)   set4 (90$_2$- -45$_2$)

set5 (-45$_2$- 90$_2$)   set6 (0$_2$- 45$_2$)   set7 (-45$_2$- 90$_2$)   set8 (0$_0$- 45$_2$)

(c)
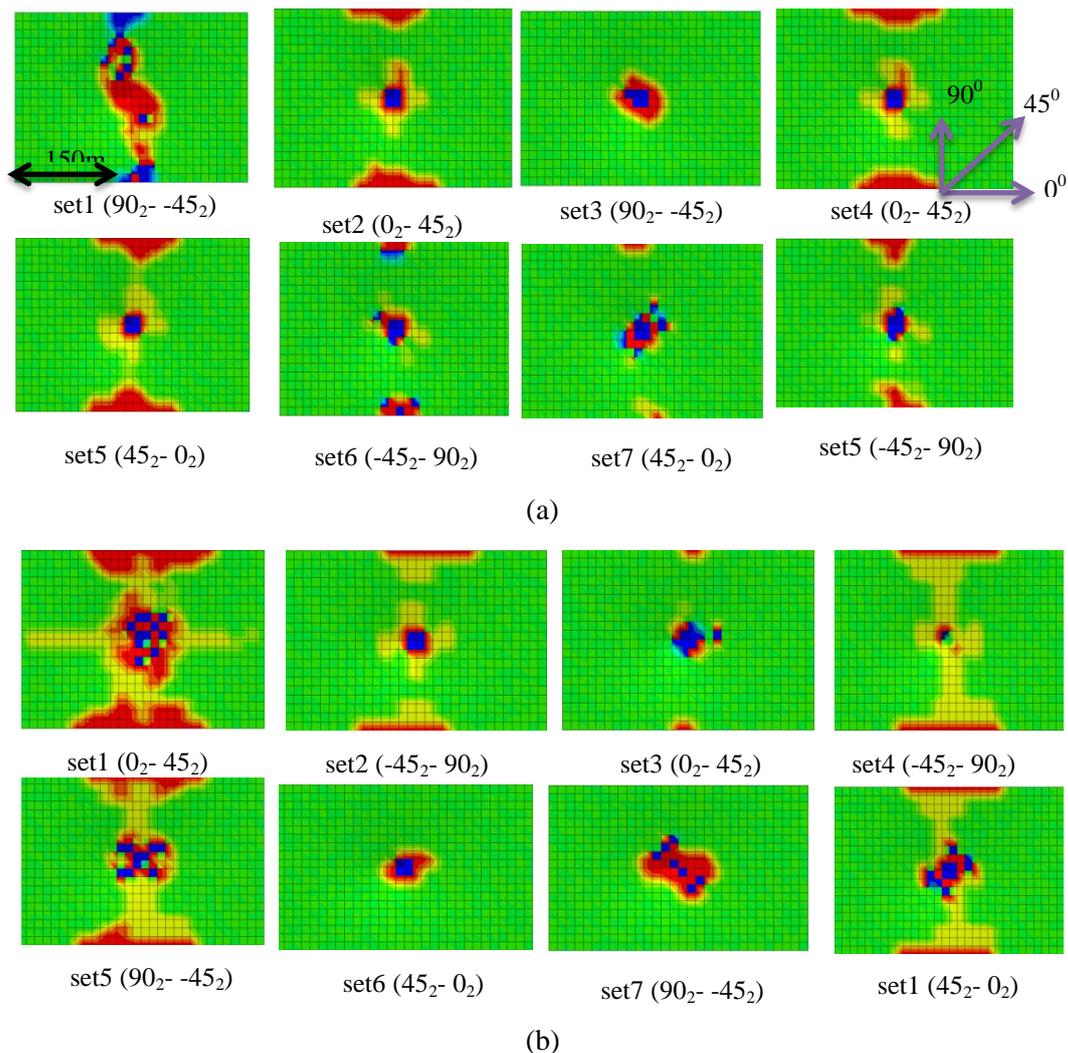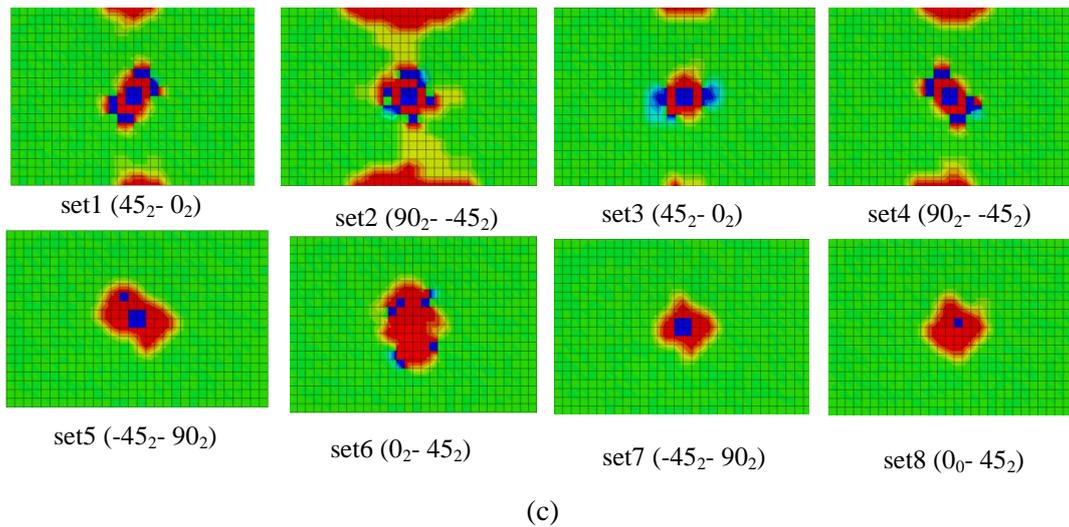
Figure 12. Matrices cracking profiles that were obtained from numerical simulation for various layers at impact energy 35 J for carbon fiber/epoxy at different layups (a)(A [90$_2$, -45$_2$,0$_2$, 45$_2$]$_{2s}$) , (b)(B [0$_2$, 45$_2$,-45$_2$, 90$_2$]$_{2s}$) , (c)(C [45$_2$, 0$_2$, 90$_2$, -45$_2$]$_{2s}$).

6. Conclusion

This paper had studied the effect of stacking sequences for composite laminates subject to low velocity impact on the failure modes. The study was experimentally and numerically. The models have implemented into commercial software FEM ABAQUS/Explicit 6.9.1 with subroutine file (VUMAT) code to build 3D model of damage redeveloped ABAQUS. Through the numerical results (delamination) comparison between the simulation results and testing results, it was a good agreement in the geometry such as shape and the area of the laminates damages (delamination). The errors percentage of damages areas for laminates through used the calculations and the statistics can be observed that errors were high at impact energy 15 J while the errors percentage has decreased at impact energy 25 and 35 J. Effect of stacking sequences is pretty clear through the results of internal energy where the internal energy of layups of A & C are greater than B at impact energy 35 J. Some oscillations have started for composites A and C in the interval of impact time of 0 s to approximate 5*10-5 s because of the elastic vibration caused by the initial contact between two surfaces of impactor and composite laminate. While the composite B, some oscillations have started in the interval of impact time of 0 s to approximate 2.5*10-5 s which presented in the total force-time histories. After that, Oscillations have stilled continued until the peak of force value that was indicated the damage initiation. Also through the results of maximum contact forces for composites which have obtained numerically that can observed that composite which layup A was stiffer than C and B which that maximum contact force is 11326.1 N for composite A at impact energy 35 J, and the maximum contact forces were 8408.075, 11004.5 N for composites B and C respectively. The results of compressive matrix cracking can be observed around the impact zone and the tensile matrix cracking is more than the compressive failure. Also it can be observed the effect of stacking sequences was clear. All damages were obtained from the numerical results need to improve with developed failure criterion.

Nomenclature

ρ	Density kg/m^3
υ	Poisson's ratio
[K]	is the stiffness matrix
[M]	is the global mass matrix

{F}	is the equivalent load corresponding to the non-linear strain because the significant deformation
{P}	is the equivalent external load corresponding to the displacement {U}
{Ü}	is the acceleration vector in low velocity impact
{U}	is the displacement vector in low velocity impact
Dα	a constant of the empirical, Choi parameter is 1.8
E_{11}	Longitudinal stiffness (GPa)
E_{22}	Transverse stiffness (GPa)
E_{33}	Out-of-plane stiffness (GPa)
f	is the impact reaction force (N)
F	single concentrated force (N)
F_m	maximum force before the unloading stage
G_{12}	In-plane shear Modulus (GPa)
G_{13}	Out-of-plane shear (GPa)
G_{23}	Out of plane shear Modulus (GPa)
K=1	Amended model considering the effect of normal stress along the thickness direction of tiered when stress in the thickness direction is positive
m	is the mass of rigid ball (kg)
n, n+1	represent the upper and lower ply
S	shear strength (MPa), 1-2.2-3.1-3 refers to i-j plane
X_c	Longitudinal compressive strength (MPa).
X_t	Longitudinal tensile strength (MPa)
Y_c	Transverse compressive strength (MPa)
Y_t	Transverse tensile strength (MPa)
α	the indentation depth (mm)
α_0	permanent indentation depth (mm)
α_{cr} , q, β,k	are experimental constants
α_m	maximum of indentation depth during the loading (mm)
β	the performance parameter, usually 2

References

[1] Al-Hadrayi Ziadoon.M.R, Zhou Chuwei "Effect the stacking sequences of composite laminates under low velocity impact on failure modes by using carbon fiber reinforced polymer" The International Journal Of Engineering And Science (IJES) || Volume || 5 || Issue || 2 || Pages || PP -53-62 || 2016 || ISSN (e): 2319 – 1813 ISSN (p): 2319 – 1805.

[2] Davies GAO, Olsson R. Impact on composite structures. Aeronaut J 2004; 108(1089):541–63.

[3] Collombet, F., Bonini, J., Lataillade, J.L., 1996. A three dimensional modelling of low velocity impact damage in composite laminates. International Journal for Numerical Methods in Engineering 39, 1491-1516.

[4] Vlot A, Kroon E, Rocca GL (1997) Impact response of fiber metal laminates. Key Eng Mat 141:235–276.

[5] Abrate S. Impact on composites structures. Cambridge Univ. Press; 1998.

[6] Berbinau P, Soutis C, Goutas P, Curtis PT. Effect of off-axis ply orientation on fibre microbuckling. Composites Part A 1999; 30:1197–207.

[7] Berbinau P, Soutis C, Guz IA. Compressive failure of 0_ unidirectional carbonfibre-reinforced plastic (CFRP) laminates by fibre micobuckling. Compos Sci Technol 1999; 59:1451–5.

[8] Her S C & Liang Y C, Compos Struct, 66 (2004) 277-285.

[9] Pinho ST, Robinson P, Iannucci L. Fracture toughness of the tensile and compressive fibre failure modes in laminated composites. Compos Sci Technol 2006; 66(13):2069–79.

[10] Abdullah MR, Cantwell WJ (2006). The impact resistance of polypropylene-based fibre–metal laminates. Compos Sci Technol 66:1682–1693.

[11] Shi Y, Swait T, Soutis C. Modelling damage evolution in composite laminates subjected to low velocity impact. Compos Struct; 2012. doi: 10.1016 j.compstruct.2012.03.039.

[12] Gonzalez EV, Maim P, Camanho PP, Turon A, Mayugo JA. Simulation of drop weight impact and compression after impact tests on composite laminates. Comput Struct; 2012. doi: 10.1016/j.compstruct.2012.05.015.

[13] F. Taheri-Behrooz • M. M. Shokrieh Iran Polym J (2014) 23:147–152 Effect of stacking sequence on failure mode of fiber metal laminates under low-velocity impact DOI 10.1007/s13726-013-0210-y.

[14] Chirangivee.K.R1, Harsha.S2, Akash.D.A3 computational analysis of effect of stscking orientation on low velocity impact behaviour GFRP composite laminate. May-2014 eISSN: 2319-1163 | pISSN: 2321-7308.

[15] Pica RDW, Hinton E. Finite element analysis of geometrically nonlinear plate behavior using a Mindlin formulation. Comput Struct 1980; 11:203-15.

[16] Tan TM, Sun CT. Wave propagation in graphite/epoxy laminates due to impact. J Appl Mech 1985; 52:6–12.

[17] Choi HY, Chang FK. A model for predicting damage in graphite/ epoxy laminated composites resulting from low-velocity point impact.J Compos Mater 1992; 26: 2134-69.

[18] Collombet F, Lalbin X, Lataillade JL. Impact behavior of laminated composites: physical basis finite element analysis. Compos Sci Technol 1998; 58:463-78.

[19] Hou JP, Petrinic N, Ruiz C, Hallett SR. Prediction of impact damage in composite plates. Compos Sci Technol 2000; 60: 273-81.

[20] Wang H, Vu-Khanh T. Fracture mechanics and mechanisms of impact-induced delamination in laminated composites. J Compos Mater 1995; 29: 156-78.

[21] Hashin Z, Rotem A. A fatigue failure criterion for fiber-reinforced materials. J Compos Mater 1973; 7: 448–64.

[22] Hashin Z. Failure criteria for uni-directional fibre composites. J Appl Mech 1980; 47(1):329-34.

[23] Li C F, Hu N, Yin Y J, Sekine H & Fukunaga H, Composites Pt A, 33 (2002) 1055-1062.

[24] ABAQUS (2003) ABAQUS/Explicit, User's Manual, Version 6.4. Hibbitt, Karlsson and Sorensen Inc., Rhode-Island, USA.

[25] ABAQUS (2003) ABAQUS, Theory Manual, Version 6.4. Hibbitt, Karlsson and Sorensen Inc., Rhode-Island, USA.